The Radial Invariance of R^2Br

Nelson Talukder

A BSc Project (SPAT) submitted to Imperial College London for the degree of Bachelors of Science in Physics.
Supervisor: Dr Robert J. Forsyth
Assessor: Dr Adam Masters
Word count: 5437

Abstract

Measurements of the interplanetary magnetic field from the Juno and ACE spacecraft were analysed around the 2013 solar maximum to compare values for R^2Br, R being the radial distance from the Sun and Br the radial component of the heliospheric magnetic field. This was determined to be a function of time and spatially invariant. Data was analysed from 2012, 2015 and 2016, with simultaneous measurements from Juno and ACE. Juno took measurements at various radial distances whilst ACE remained near the Earth at the Lagrangian point L1 allowing different radial separations to be compared. This gave the conclusion that within error, R^2Br was radially invariant, when averaged over 2 solar cycles. R^2Br was taken for both the negative and positive sectors to allow for a better comparison. The suitability of a standard time period of switching between the negative and positive directions of the magnetic field as a comparison for R^2Br was assessed. This was shown to be inconsistent when measured near the solar maximum as was the case in 2012, 2015 and 2016 due to the deviation from a periodic variation expected from a rotating dipole over a rotation period.

Acknowledgements

I would like to thank my supervisor Dr Robert Forsyth and my assessor Dr Adam Masters. Additional thanks go to Emma Davies for providing the data used within this report and Dr Simon Good for his insight.

Contents

1. Introduction and Aims

NASA is expected to launch a spacecraft in July 2018 that will be the first named after a living scientist [1]. The Parker Solar Probe, named after Eugene Parker, a pioneering researcher in space physics, is expected to reach the Sun's atmosphere where it will gather new data, to fuel more theories and deepen our understanding of the surface of our local star. In this investigation, solar effects will be considered at distances far beyond the solar surface, including the interplanetary magnetic field between the Earth and Jupiter.

Eugene Parker's paper, 'Dynamics of the interplanetary gas and magnetic fields' [2] covers much of the theory used in this investigation including the effect of the solar wind on the shape and magnitude of the heliospheric magnetic field (HMF). As the solar wind was a relatively new idea at the time, having only recently been proposed [3], the concept was somewhat idealised and significant cases of deviations from the Parker solar wind model have been observed, including to the direction of the magnetic field [4].

Current research often uses the Parker solar wind Model as a first approximation with which to compare magnetic field observations. Measurements by Voyager 1 and 2 of $|B|$, the magnetic field magnitude, have been found to be consistent with the Parker solar wind model [5] at radial distances up to 86 AU. This is far beyond the distances used within this investigation and demonstrates the validity of a similar approach for use in distances up to 5.4 AU, such as those considered here, when analysing the effect of the solar wind on the magnetic field strength. This investigation attempts to verify the radial invariance of R^2Br in the ecliptic plane via observations of the time variation of R^2Br at different radial distances from the Sun.

HMF measurements used in this investigation came from the Juno and ACE (Advanced Composition Explorer) spacecraft, which were analysed by year. The time periods considered were the years 2012, 2015 and 2016 where Juno was separated by a range of distances from ACE. This enabled comparison of the magnetic field over a range of radial distance from 0.6 AU to 4.4 AU. 2013 and 2014 were not analysed to avoid the additional solar activity during solar maximum such as the reversal of the magnetic pole, which sees a major change in the coronal magnetic field [6] to include quadrupole and even octopole behaviour.

The dipole nature of the Sun was also examined to check the best timescale over which to average time variations in the HMF. This was to test if a similar periodic variation in the HMF could be observed at ACE and Juno as the direction of the HMF switched between the positive and negative sectors.

2. Theory

The investigation considers whether an inverse square law is a sufficient model for the decrease in the magnetic field from the foot of the magnetic field lines at the solar surface to any radial distance, R which is greater than 1 AU. Changes to the strength and direction of the magnetic field due to the solar wind flow had to also be taken into account. This required a model of the variation of the field according to the Parker spiral that took into account any changes to the measured field strength due to the rotation of the Sun.

Previous investigations into the time variation of an individual sector of R^2Br included the work by Smith and Balogh in 1996 [7]. Here measurements of the negative sector of Ulysses at different latitudes were analysed alongside constant latitude measurements by IMP-8, which remained in the ecliptic plane. A comparison of measurements for IMP-8 and Ulysses, between 1992 and 1996, can be seen in Figure 2.1.

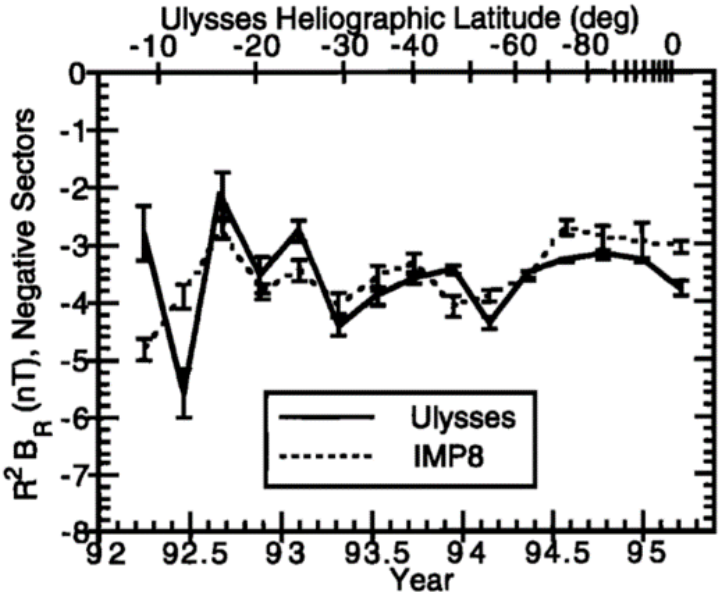

Figure 2.1: Smith and Balogh [7], radial invariance for a range of latitudes

The investigation showed that at different positions to the Sun, the value of R^2Br were very similar, suggesting R^2Br was latitude invariant. This investigation aimed to use a similar approach such as averaging over multiple solar cycles to compare data from spacecraft separated by distances between 0.6 and 4.2 AU. A notable difference is this investigation used both the positive and negative sector, using measurements from ACE and Juno in the ecliptic plane.

2.1 Magnetic dipole

Electric currents in the Sun produce a magnetic field within the Sun as shown by Dynamo theorem [8]. If the solar magnetic field was dipolar, the expectation would be a $1/r^3$ fall off in field strength with radial distance, following a standard dipole field, however this is not the case. The solar wind drags out the magnetic field lines resulting in a significantly altered structure. This report seeks to determine the validity of using an inverse square law to model the decrease in the magnetic field for each sector. The general trend for $|B|$ has previously been observed to follow a power law with an index between -1.67 to -2.3 [9].

Br, the radial component of the HMF, is used here due to predictions [2] that the magnetic field is radially outward near the solar surface at about 2.5 solar radii, shown in Figure 2.2. The reasoning being the solar wind drags out the magnetic field lines to be approximately normal to the surface of the Sun. Any change to the direction of the magnetic field will therefore be due to solar rotation, the radial component will continue to represent the field at the solar surface, taking into account power law decrease in magnitude.

The magnetic field of the Sun can be defined as either inward or outward, due to the loop like nature of the field lines. This allows the field to be defined as being in the negative sector for field lines that point inwards and positive for field lines that point outwards.

The tilt of the Sun in the ecliptic plane means that as the Sun rotates, the outward field lines from the upper hemisphere of the Sun and the inward field lines from the lower hemisphere of the Sun can be measured as was the case for solar cycle 24 [7]. The inward and outward directions of the field change orientation roughly every 11 years with the solar cycle due to the change in the direction of the solar dipole so the outward field lines originated from the lower hemisphere in cycle 23. There should be at least 1 observation of each sector per solar rotation due to the basic tilted dipole structure, however further switching could be expected due to a significant deviation from a clear dipole as well as the reduction in the dipole behaviour expected near solar maximum. An alternative way to think about this is through the heliospheric current sheet, where an object in the ecliptic plane could be expected to cross it twice over a solar rotation producing a periodic variation.

2.2 Frozen In Theorem and the Parker Spiral

The plasma of the solar wind is able to drag out the magnetic field lines due to the excellent electrical conductivity of the plasma resulting in the magnetic field lines being frozen into the solar wind. The solar wind flows radially outward from the surface of the Sun [6] and as the Sun rotates the stream of plasma keeps flowing radially whilst the magnetic field, which remains continuous, has to spiral around the Sun to thread all the plasma parcels which originated at the sun at the foot-point of the magnetic field line. This, along with frozen in theorem, leads to magnetic field lines with a direction that points at an angle to $\hat{R}$ as shown in Figure 2.2. Measurements of the field were taken in three spatial directions using the Radial-Transverse-Normal (RTN) system with $\hat{R}$ defined as the direction radially away from the sun $\hat{T}$ defined using the angular frequency of the Sun, $\mathbf{\Omega}$, the distance of the object from the Sun, $\mathbf{R}$,

$$\hat{\mathbf{T}} = \frac{\mathbf{\Omega} \times \mathbf{R}}{|\mathbf{\Omega} \times \mathbf{R}|} \tag{2.1}$$

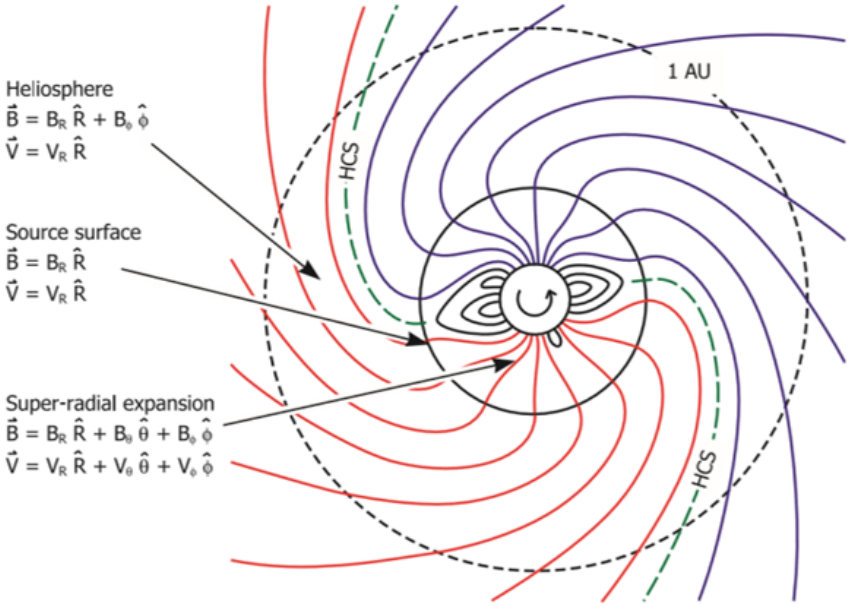

Figure 2.2: The Parker spiral, as viewed from above, with $\hat{N}$ out of the page. This is in the non rotating solar frame.

and $\hat{N}$ normal to $\hat{R}$ and $\hat{T}$. The outward magnetic field had to be determined from the angle of the magnetic field and its magnitude from the B_r component.

The angle of the Parker spiral to $\hat{R}$, angle Φ_P could be calculated from Ω, R and the speed of the solar wind, V_R by

$$\Phi_P = -\arctan \frac{\Omega R \sin\theta}{V_R} \tag{2.2}$$

As both spacecraft remained near the ecliptic plane the angle of the object, for which $\theta \simeq 90°$ and $\sin\theta \simeq 1$.

2.3 Solar Wind Turbulence

The measurements made by Ulysses in 1992 to 1995 were of high latitudes where the fast solar wind, approximately 700km s^{-1}, is dominant [7]. Comparatively Juno and ACE made measurements of the ecliptic plane where the slow solar wind with an average velocity of 400km s^{-1}, is dominant. The slower wind speed increased the turbulence within the solar wind resulting in a more tangled set of field lines as would be suggested by Frozen in Theorem. This meant the negative and positive sectors were not as well defined for Juno and ACE as for Ulysses.

Extra fluctuations on a longer timescale between outward and inward field directions could be introduced due to differential rotation, where the rotation velocity of the Sun varies with latitude, and meridional circulation, where the ion move in polar directions [8]. This presents extra fluctuations in the data as the field lines originate from different areas of the Sun. This leads to the new areas of the Sun producing a magnetic field lines, causing a change in the direction observed much further out from the Sun.

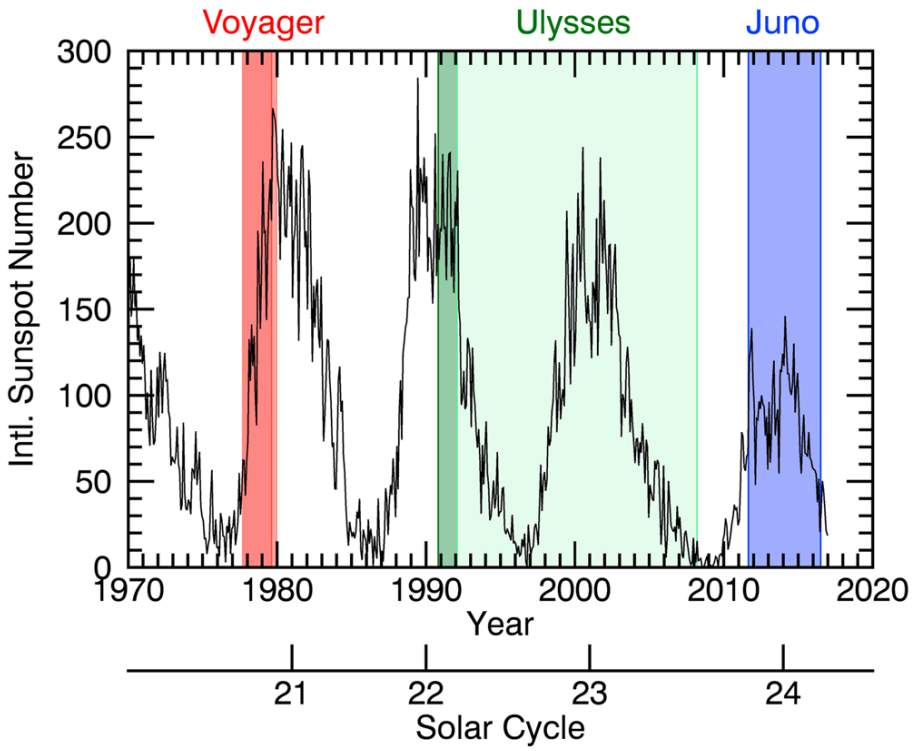

[H]

Figure 2.3: Sunspot number observed over solar cycles 21 to 24, Gruesbeck [9]. Juno took measurements over the maxima of solar cycl e 24, where sunspot number counts were significantly lower than any maxima from the past 50 years.

2.4 Sunspot activity

Sunspots are where the magnetic field emerges at the solar surface. Therefore they theoretically correspond to the strength of the field lines originating from that region of the Sun. Sunspots are often taken to be the measure of solar activity as they follow the 11-year cycle in solar activity.

There has been a significant decrease in the average number of sunspots over the previous 3 solar maxima, as shown in figure 2.3 [9]. This can be verified to see if there has also been a significant decrease in the strength of the magnetic field as produced by the Sun. This can be carried out by comparing the values of R^2Br for different solar cycles.

3. Method

3.1 Data Handling

The HMF measurements were available for each spacecraft for 2012, 2015 and 2016. The magnetic field values were provided averaged over 1 minute for Juno and 4 minutes for ACE as the three vector components of the magnetic field using the RTN system. Further information was also provided on the location of the spacecraft relative to the sun for Juno and relative to the Earth for ACE which could be used to evaluate R^2. The data was handled in Python, where it was converted into Pandas DataFrames, this package provided a convenient method of plotting, selecting and averaging data. An overview of the complete programme can be seen in Figure 3.1.

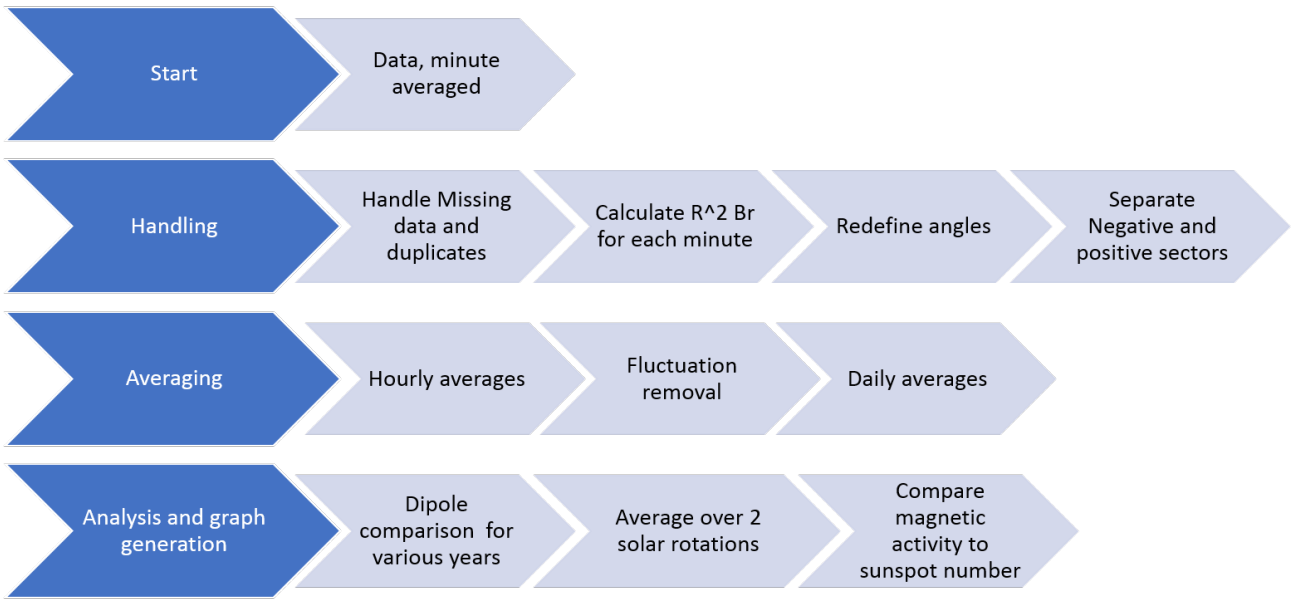

Figure 3.1: The method used to get data for analysis of R^2Br

3.1.1 Missing data and duplicates

There were occasions where data was not available for particular minutes or for a long sequence of time. This was an issue in all six data sets as it meant that the programme would either consider the HMF measurements as 0 or it would interpolate the data when plotting. To counter this problem, an inbuilt function of the Pandas package was used which could add extra, empty rows to the dataset for any missing minute or 4 minute periods, with an indication that the position and HMF measurements were missing for this particular period. Another issue was with duplicates in the data, this was rare with the most being 5 duplicate minutes for Juno in 2015. The disruption caused to the programme by duplicate data however meant a method to locate and remove 2 data entries for the same time was implemented, keeping the first instance for the time period.

3.1.2 Daily and Hourly averages

The data was averaged into hourly periods and any missing hours within the data was included as 'NaN' values to make sure further data analysis would not consider data from missing sections. This also allowed discontinuities in any graphs for where not data was available. The 2012 data from Juno included a 25 day gap where no measurements were available, this caused the gap in Figure 3.2 between days 237 and 262. This highlighted the need to find a method to process missing data. Daily averages were calculated after the hourly averaged data was separated into positive and negative sector measurements. Additionally, the programme considered days with a significant mix between measurements from either sector. The daily averaged data allowed for much clearer observation of general trends and made it much more comparable to sunspot numbers, which were provided daily.

Errors

Errors values used were the statistical error calculated as 2 standard deviations. This was recalculated depending on the averaging time from hourly, daily up to 2 solar rotation periods.

Figure 3.2: Daily averages, the error is given in green

3.1.3 Separation of negative and positive sectors

The angle of the outward and inward magnetic field was determined so the negative and positive sectors could be isolated. The angle used to separate the sectors was the angle to the $\hat{R}$ vector, Φ_B, defined as

$$\Phi_B = \arctan \frac{B_t}{B_r} \tag{3.1}$$

Φ_B was calculated for each measurement in the dataset as it was predicted to vary with radial position from the Sun as predicted by the Parker Model. By subtracting $\Phi_B - \Phi_P$, analogous to moving the data to a new coordinate axis from the plane $\hat{R}\hat{T}$ set up to $\hat{R}'\hat{T}'$, the range of angles corresponding to the new sunward and anti-sunward directions were determined, separating the data according to their sector.

Errors

There were fluctuations between the sectors, for angles by the boundary where the magnetic vectors could have been negative or positive within error. This was caused by stochastic effects in the turbulent plasma, removing them meant there could be a clear separation between the negative and positive sectors. To remove this effect from the data, measurements within the theoretical error of 1.3°, calculated from equation (3.2) were removed from averaging.

Error in the angle was calculated using the propagation of errors formula. This assumed an error in the speed of the solar wind of $\sigma_{VR} = 50\text{km s}^{-1}$. The error in the measurement of the radial distance was negligible so was not used in the error calculation. There was a significant contribution from the error in the angular frequency of the solar rotation due to a solar rotation

error which previous work [10] suggested could be up to $\sigma_\Omega = 0.25$ days in the ecliptic plane. This was rearranged to equation (3.2).

$$\sigma_{\phi p} = \left(\frac{1}{1+\left(\frac{\Omega R}{V_R}\right)^2}\right)\left(\left(\frac{\Omega R}{V_R^2}\right)^2 \sigma_{VR}^2 + \left(\frac{\Omega R}{V_R}\right)^2 \sigma_\Omega^2\right)^{\frac{1}{2}} \tag{3.2}$$

3.1.4 Days with a switch in polarity

R^2Br was averaged over 24 hour periods to obtain a clearer comparison between the values obtained at ACE and Juno. 94 days did however have a sector switch for ACE in 2012 where there was at least 1 hour per day with the opposite polarity and this was similar for other years. To deal with this, it was required to find out the proportion of each day spent in either sector to determine if it contributed significantly to the average R^2Br value for that particular day. This was included in the fluctuation reduction, where days in which there were 6 hours or less from one sector compared were averaged just over the dominant sector. It was noted the majority of of switches in magnetic field orientation were for fewer than 6 hours. As this meant less than 25% of the day was spent in a different sector, these days were averaged across the dominant sector. Therefore far fewer days, 34 for ACE, had to be excluded when separating the data into two different set of days according to the positive and negative sectors. The histogram of the hour sequences, Figure 3.3, shows that the number of isolated sequences between 1 and 6 hours could be completely removed from with a condition. This condition was days with fewer than 18 hours in the dominant sector or sequences removed due to not contributing a total of 6 hours of the non-dominant sector to that day. This showed that random switches could be removed without significantly affecting the daily average due to them being well spread out over each year and only contributing a small amount to each day.

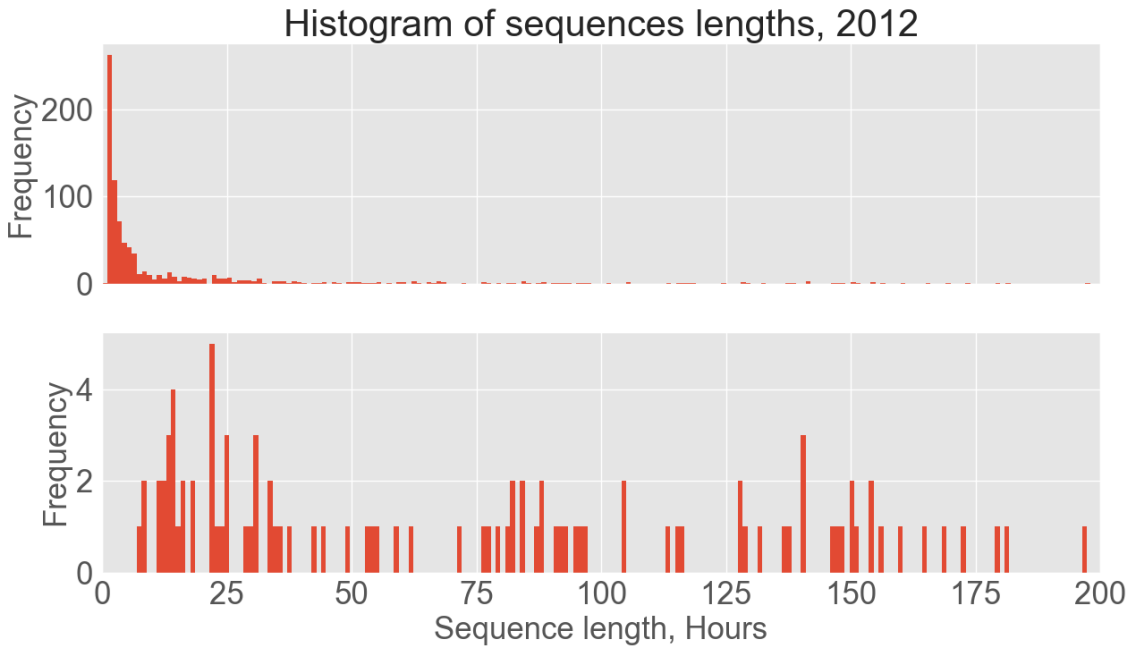

Figure 3.3: ACE 2012, the majority of hourly switches between negative and positive sector were very short. Removing these as shown in the lower panel, meant removing almost all short fluctuations that were less than a day in length.

3.2 Data analysis

3.2.1 Averaging over multiple solar cycles

It was decided to average over 2 solar periods with the expectation [8] that shorter fluctuations would average to the same value for both ACE and Juno. This would remove the effect of shorter-term contributions to the magnetic field, such as the effect of CME's which are not longitudinally invariant due to occurring locally on a particular section of the solar surface. The resultant plasma which then propagates only covers a range of azmithul angles. As several CME's are expected to be present in the data over each solar rotation period, it is expected they contribute a similar amount to total the measurements of Br for each rotation period. For the comparison between IMP-8 and Ulysses, Smith and Balogh used 3 solar cycle however 2 solar cycles was sufficient here and allowed for more data points.

3.2.2 Identifying CIR signals

To check on The measurements were checked separately for a CIR pattern by plotting $|B|$ for periodic increases in the magnetic field strength above the expected average. $|B|$ was contrasted day by day on a scale that took into account the maximum of the data as the maximum of the scale to allow for spikes from the standard background to be compared. Measurements were compared in stages of 180 days as only 180 days of data were usable for 2016. Additionally, the value of $|B|$ could be compared with more precision due to finer detail for each time period.

3.2.3 Sunspot activity

Sunspot data was provided by the Royal Observatory of Belgium. This was averaged over 50 days and plotted as a bar chart, with the height of the bars providing the average daily sunspot number and $|B|$ was plotted on the same axis. The data was placed in bins of the daily estimates of the total sunspot number based on real observation. The value for the magnitude $|B|\,R^2$ was used to compare the magnitude of the HMF to the sunspot count. The aim of this was to check if short term trends in the sunspot number reflected the time variation in the HMF as would be the case if the strength of the magnetic field depended only on solar activity.

4. Initial Findings

4.1 Radial Distance

The graph of the radial distance of Juno from the Sun, Figure 4.1 showed that the spacecraft did not travel steadily outwards to Jupiter. Juno first travelled out to 2.3 AU before returning to 1AU due to a gravity assist from the earth in October 2013. This showed there was some overlap in the radial distances covered, meaning either 2012 or 2013 could be excluded. It can also be seen the range of distances covered during 2012, 2015 and 2016 included 1 to 2.3 AU and 4 to 5.4 AU.

2013 and 2014 were both at solar maximum, according to the sunspot data in Figure 2.3 and therefore included the effect of the evolution away from a magnetic dipole that occurs during solar maximum, leading to a more complex magnetic field structure. This was the main reason for their exclusion.

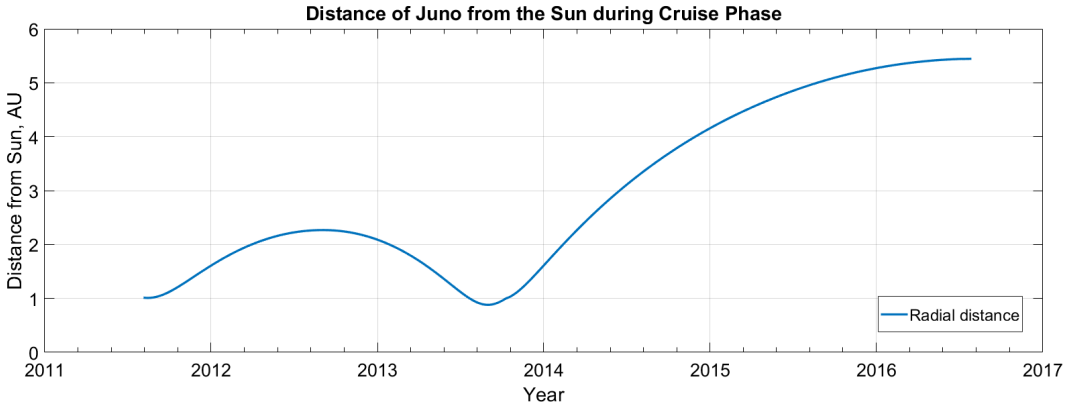

Figure 4.1: Radial Distance of Juno from the Sun

4.2 Angle

Using Equation (2.2), yielded a value of $-45°$ for ACE. Measurements by ACE, shown in Figure 4.2 were in agreement with this prediction, with a peak in the number of magnetic vectors at $-50°$. The distribution is due several processes that could alter the direction of the field including CME's and long duration non-Parker spiral intervals[11], which results in a continuous range of angles of the field. Within error, the peak of the range followed Equation (2.2). The minima in Figure 4.2 indicated where the separation between the sectors occurred. The angle was at the very edge of the accepted error suggesting there could be other effects

which caused deviations from an ideal Parker spiral. A suggested mechanism could be due to co-rotating rarefaction regions, CRR's. In Ulysses observations[4], CRR's were found to cause deviations of up 30° from the Archimedean spiral, for several days. This could have shifted the peak substantially.

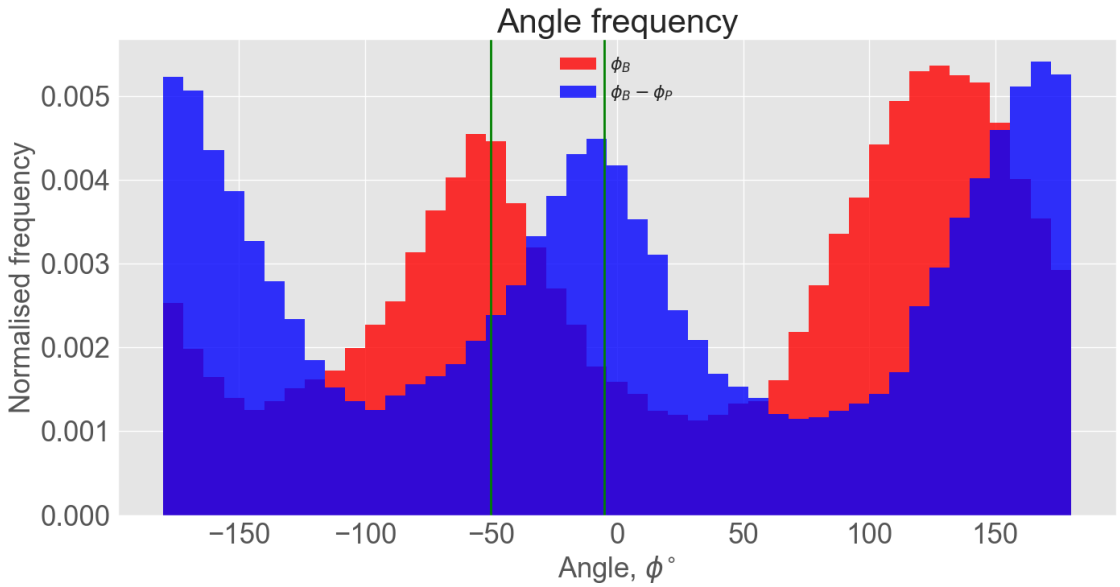

Figure 4.2: The normalised frequency of different magnetic vectors for ACE in 2012, separated into bins of 10°. ϕ_B is the angle of the magnetic field to $\hat{R}$ vector with $\phi_P = 45°$ as the angle of the Parker spiral to $\hat{R}$. Correcting the allowed $\phi = 90°$ to represent the positive sector and $|\phi| > 90°$ to be the positive sector. The green lines indicate the transformation of sunward and anti-sunward from $\hat{R}$ to $\hat{R}'$ by rotating the system by ϕ_P

4.3 Dipole comparison

Comparing the dipole signature of ACE and Juno was proposed as a method to verify if the time variation at the two spacecraft was indeed the same. If a similar function that was periodic with each solar rotation could be identified it could be used to compare the time variation of the HMF. This also assumed the magnetic field measured was consistent with a rotating dipole, where the HCS is crossed twice per solar rotation by each Space probe. 2012, however, was near the solar maximum where the magnetic field of the Sun is more representative of a quadrupole or octopole.

Variations in the solar wind occur with the solar wind which introduced a time lag where the solar wind reached ACE up to 13 days later [8], which would have to be taken into account with this approach. This approach expected periodic switch between the positive and negative sector that was half a solar rotation period, or 12.65 days for Juno and 13.5 days for ACE.

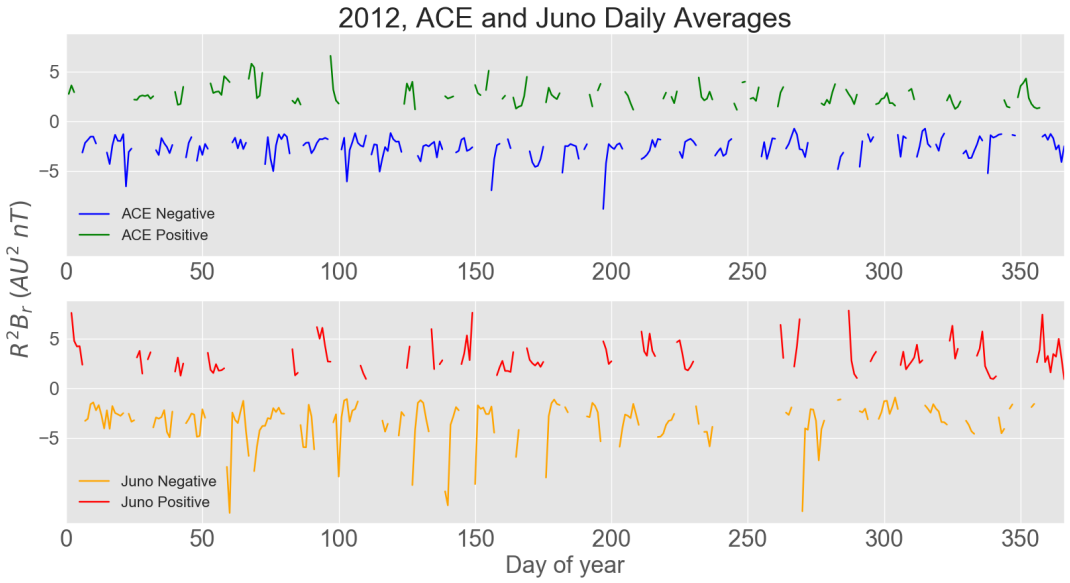

Figure 4.3: Switching between the positive and negative sector for ACE in 2012

Comparatively, 2016 gave a much more consistent dipole switching period, however this was not able to give a definite overlap for the ACE and Juno as shown in Figure 4.4. By this point Juno was close to Jupiter so data that was affected by the space probe entering the Jovian bow shock had to be discounted for Juno.

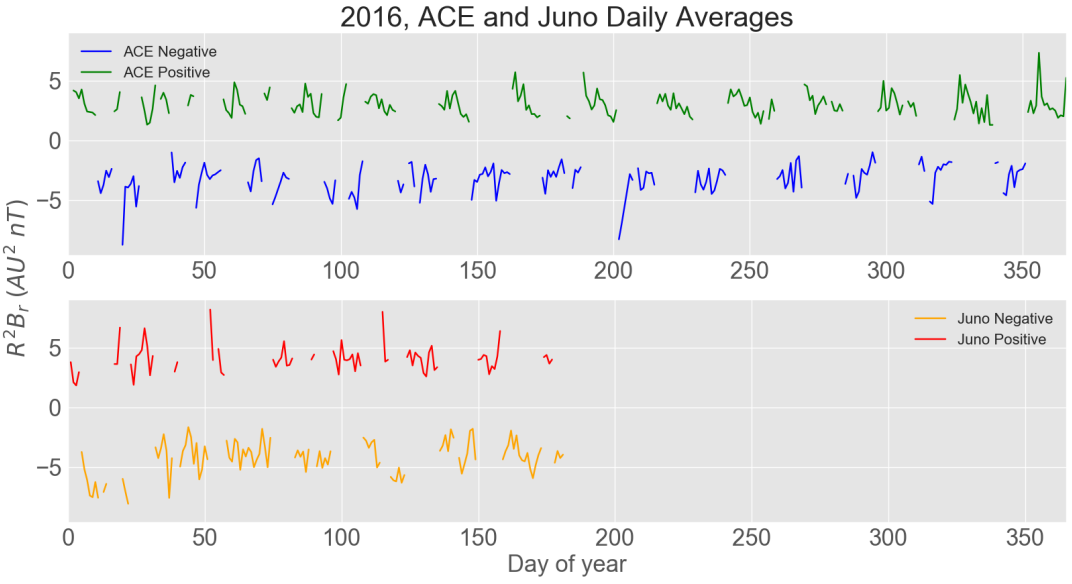

Figure 4.4: 2016, comparing the dipole nature at ACE and Juno

Attempts to refine the data, including signal processing to remove other frequencies of fluctuations that were not able to retrieve a comparable result for ACE and Juno. It was concluded there was too significant a deviation from a pure dipole for 2012, 2015 and 2016 to compare longitude variation at ACE and Juno. From here, it was decided to suppress any longitudinal variation by averaging over longer time periods than a single day.

5. Results and Discussion

Averaging over one or more solar cycles meant the longitudinal dependence of the time-varying magnetic field could be averaged out, the need for this was demonstrated by the daily averaged values of R^2Br, which exhibited fluctuations over timescales much less than the solar rotation period. This gave the conclusion that Br needed to be considered for all azmithul angles to exclude longitude dependent events such as CMEs, which increased R^2Br for particular days as highlighted by Figures 4.3 and 4.4. 2 solar rotation periods were used to allow the longitudinal dependency to be sufficiently suppressed, whilst still having a significant number of set points to allow for a comparison of time dependence.

5.1 R^2Br over 2 solar cycles

The average magnitude of the negative sector of the HMF found by Smith and Balogh was -3.5 AU^2nT [7] for Ulysses and IMP-8. This was similar to the negative sector measurements for ACE and Juno, shown in Table 5.1. These measurements were made during the declining phase of Solar cycle 22 from 1992 to 1995 and could be compared to 2015 and 2016, which covered the declining phase of cycle 24. The value was slightly lower for 1992-1995 compared to 2015-2016 with both being directly after solar maximum according to Figure 2.3. 2015-2016 was however close to a solar maximum, whereas the measurements for 1992-1995 were across 4 years, leading to contributions from years further from the solar maximum reducing the average.

There was a difference in scale of the data used by Smith and Balogh [7] compared to the data used in this investigation. The averages given in their article were of a much wider range so that despite latitude invariance, the data will have included a greater evolution of the magnetic field. Comparing the negative sector from one investigation to another had limited results. This was due to varying contributions to measurements of the negative sector for different periods, and meant no clear decline in magnetic field strength could be observed over 2 solar cycles.

	ACE (AU^2 nT)	**Juno** (AU^2 nT)
2015	-3.5	-4.5
2016	-3.2	-4.5

Table 5.1: Negative Sector averages of R^2Br for 2015 and 2016

5.2 Radial invariance of R^2Br

The relation obtained in Figure 5.1 shows that within error, the value of R^2Br was spatially invariant, with the overall trend being followed across 2012, 2015 and 2016.

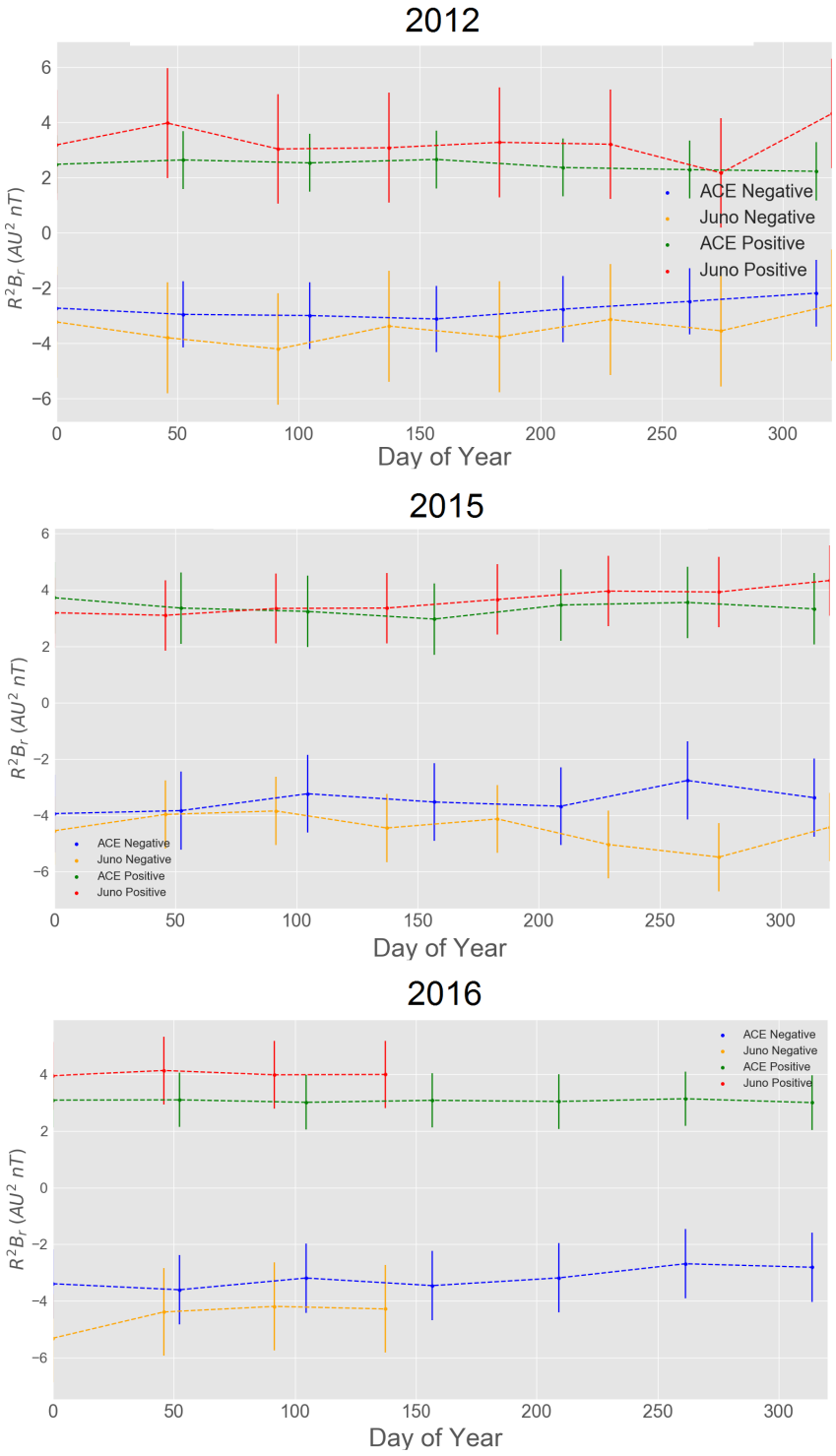

Figure 5.1: R^2Br for 2012, 2015 and 2016. Averaged over 2 solar rotation periods of 50.6 days for Juno and 54 Days for ACE.

2016 saw a significant increase in the difference in the field strength of the HMF observed by Juno compared to ACE however was still within error. This increase could be the result of increased flux from coronal holes, creating and sustaining an increase for a significant proportion of the year. Coronal holes are relatively stable structures located on the solar surface so can act as a source of magnetic flux for up to a year [6].

There was a greater standard deviation in the measurements by Juno for 2012. This was expected due to the measurements being taken over a time period closer to solar maximum where an increased variation in the magnetic field strength was expected at distances further from the Sun [12]. 2015 and 2016 were further from the maximum so observed fluctuations had a lower average amplitude.

2012 was before the solar maximum whilst 2015 and 2016 were after. This meant measurements were taken of the opposite polarities of the Sun. Previous investigations [8] have highlighted that CIRs appear more common to the declining phase of the solar cycle as solar activity reaches a minimum, as was the case for 2015 and 2016.

5.2.1 Co-rotating interaction regions

CIR are expected near the solar minimum due to the direction of the magnetic dipole being more aligned with the rotation axis. This results in more balanced contribution from both fast solar wind from higher latitudes and the slow solar wind from the equator leading to a higher chance of of compression regions forming between the two types of solar wind[13]. This allows for an increase in the magnetic field strength leading up to the solar minimum, as the tilt in the solar magnetic dipole approaches the axis of rotation, expected for 2015 and 2016.

CIRs are known to be caused by a compression of the slow and fast solar winds resulting in a periodic increase in magnetic field strength. The regular increase in $|B|$ over the 25-27 day solar rotation period contributed significantly to the average. Previous observations from Ulysses of the HMF have shown an enhanced magnetic field strength up to several times the average[14].

As the source of the fast solar wind, the stability of coronal holes influence the duration of any resultant CIRs. Very stable coronal holes enable CIRs to be sustained over several solar rotation periods [15]. This means one or more averaging periods used in Figure 5.1 could have an enhanced magnetic field strength leading to a higher than expected value for R^2Br. Unlike ICME contributions, CIR contributions cannot be averaged over multiple solar rotations as they occur much more infrequently and for only specific periods of the year. No previous research has been published verifying if Juno has encountered CIR behaviour. The scale of the increase suggests very stable CIRs [8] are a possible mechanism causing higher than expected magnetic field strengths.

Measurements from Juno in 2016 showed some sign of periodic increases in $|B|$ as shown in Figure 5.2. There were peaks with maxima greater than 2nT, higher than expected when compared to 2015 data. Therefore it was concluded something other than CMEs could be causing fluctuations in the magnetic field strength. Between days 16 and 85 in Figure 5.2, there were 2 increases in $|B|$ every solar rotation which would be expected from a CIR. After day 85 the signal was disrupted by CME signals. This suggests stable coronal holes contributed to producing a fast solar wind capable of causing compression region and maintaining it for at least 2-3 solar rotations. Figure 5.2 showed that 2012 and 2015 also did not display a similar periodic increase in $|B|$ identified in 2016.

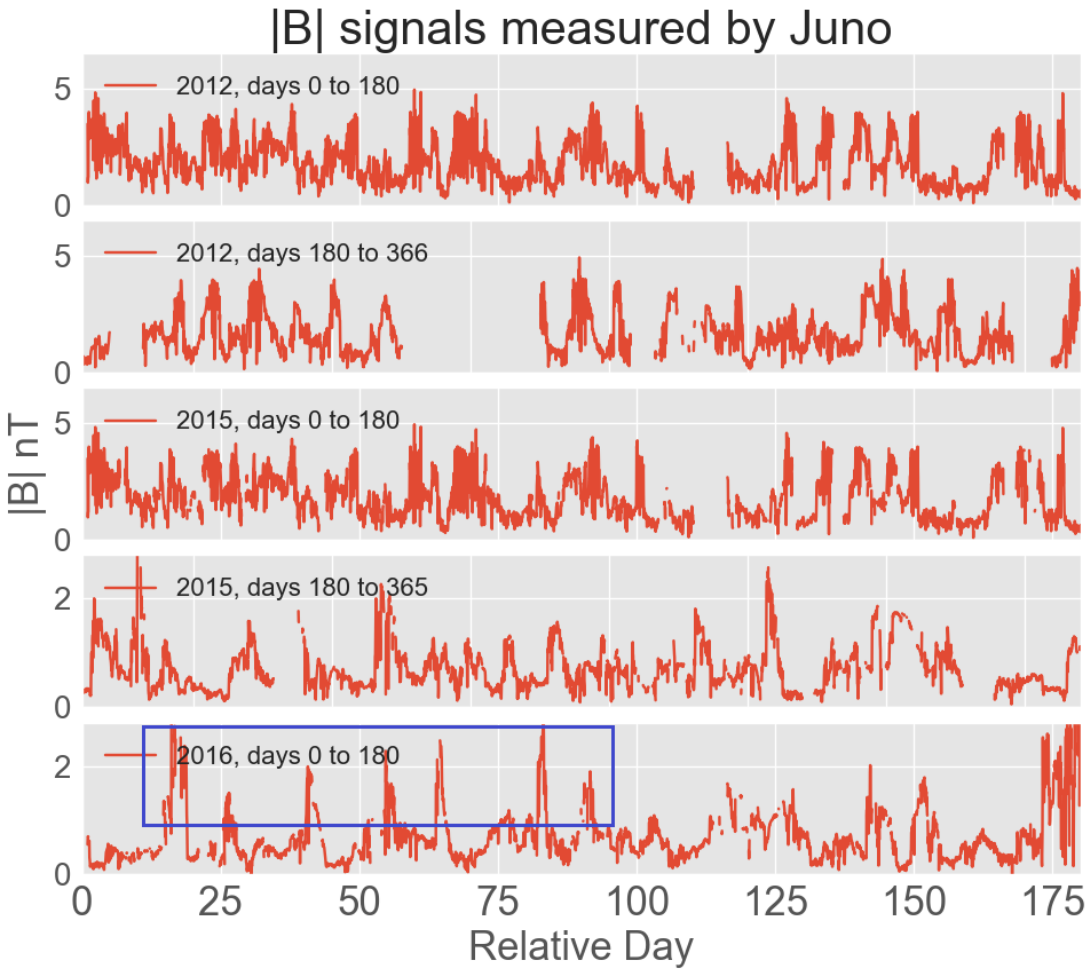

Figure 5.2: Comparing CIR signals over 180 days in 2012, 2015 and 2016 for Juno. 2 events per solar rotation were visible for 2016 for days 16-85, in the blue box in the lower panel. CME signals disrupted the pattern later in 2016.

Wind speed data was not available to verify if slow and fast solar winds were encountered in the ecliptic plane by Juno. If regions of fast and slow solar wind were in contact if the fast and slow and solar wind speeds were measured with a characteristic variation over the 25-27 day period of the rotation it would provide further evidence a CIR was encountered by Juno.

A further factor is that contrary to the general decline in daily sunspot number, $|B|$ increased for 2016 and remained higher than the comparative sunspot count would suggest. This suggests that plasma compression rather than solar activity caused an increase in magnetic field.

5.3 Sunspot number

The sunspot number was plotted against R^2Br, Figure 5.3, to directly compare solar activity against the strength of the magnetic field.

This showed the magnetic field, as measured by Juno in 2016, remained particularly high

despite the decrease in sunspot activity. This was indicated by the reduction in sunspot number not being as closely correlated to the observed magnetic field strength as would be expected for the declining phase of the solar cycle, indicated in Figure 2.3. Additionally Figure, 4.4 showed 2016 had clear signs of a periodic crossing of the HCS by Juno, a requirement for a HCS consistent with a well defined solar dipole [16]. It has been observed that the Sun is almost like a magnetic dipole near a solar minimum indicating 2016 was far closer to a solar minimum.

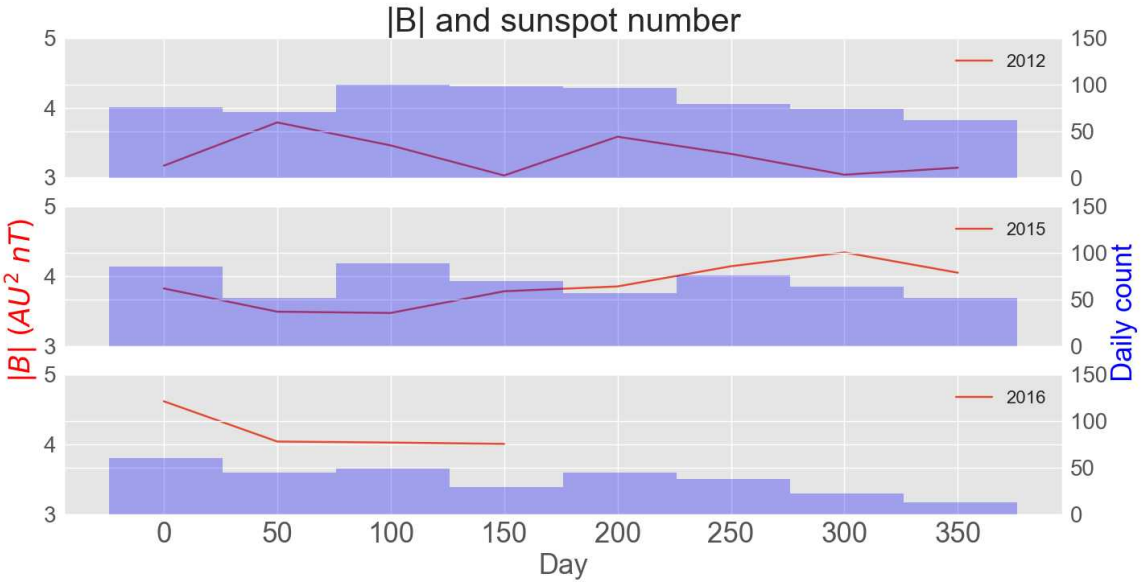

Figure 5.3: Comparing the variation in sunspot number to the change in the magnetic field on a smaller scale, for Juno. The data was averaged for 50 days periods.

6. Conclusion

Within error, R^2Br was spatially invariant in the ecliptic plane for 2012, 2015 and 2016 with the same variation found for both Juno and ACE with CIR effects accounting for any deviations. This suggests that inverse square law is still a relevant first order approximation for the time variation of the positive and negative sectors of R^2Br.

The magnetic dipole properties of the Sun were found to be unsuitable for comparing the time variation of R^2Br due to short variations in magnetic field that were longitudinally dependent. The scale of the switching of the negative and positive sectors in the ecliptic plane of 13.5 days for ACE and 12.65 days for Juno was too small a scale to discount the effect of CMEs.

Further investigation could check if 2013 and 2014 may be analysed to see if the same approach is valid during the reversal of polarity of the HMF at solar maximum. This, however, would require further research into the activity that occurs around solar maximum and the effect this has on the magnetic field.

Bibliography

[1] R. Garner. Parker Solar Probe, 2017. https://www.nasa.gov/content/goddard/parker-solar-probe.

[2] E. N. Parker. Dynamics of the Interplanetary Gas and Magnetic Fields. *Astrophysical Journal*, 128:664, 1958.

[3] L. Biermann. Solar corpuscular radiation and the interplanetary gas. *The Observatory*, 77:109–110, 1957.

[4] N. Murphy, E. J. Smith, and N. A. Schwadron. Strongly underwound magnetic fields in co-rotating rarefaction regions: Observations and Implications. *Geophysics Research Letters*, 29:2066, 2002.

[5] Richardson J. D., C. Wang, and C. F. Burlaga. The solar wind in the outer heliosphere. *Advances in Space Research*, 34:150 – 156, 2004.

[6] R. J. Forsyth and M. J. Owens. Review Article. *Living Reviews in Solar Physics*, 10:5, 2013.

[7] E. J. Smith and A. Balogh. Ulysses observations of the radial magnetic field. *Geophysics Research Letters*, 22:3317–3320, 1995.

[8] J. T. Gosling. *Heliophysics*. Cambridge University Press, 2010.

[9] J. R. Gruesbeck, D. J. Gershman, J. R. Espley, and J. E. P. Connerney. The interplanetary magnetic field observed by Juno enroute to Jupiter. *Geophysics Research Letters*, 44:5936–5942, 2017.

[10] F. Ward. Determination of the Solar-Rotation Rate from the Motion of Identifiable Features. *Astrophysical Journal*, 145:416, 1966.

[11] J. E. Borovsky. On the variations of the solar wind magnetic field about the Parker spiral direction. *Journal of Geophysical Research (Space Physics)*, 115:A09101, 2010.

[12] S. K. Solanki, B. Inhester, and M. Schüssler. The solar magnetic field. *Reports on Progress in Physics*, 69:563–668, 2006.

[13] V. J. Gosling, J. T.and Pizzo. Formation and Evolution of Corotating Interaction Regions and their Three Dimensional Structure. *Space Science Reviews*, 89(1):21–52, 1999.

[14] R. J. Forsyth and J. T. Gosling. *Corotating and transient structures in the heliosphere*, pages 107–166. 2001.

[15] I. G. Richardson. Solar wind stream interaction regions throughout the heliosphere. *Living Reviews in Solar Physics*, 15(1):1, 2018.

[16] T. R. Sanderson, T. Appourchaux, J. T. Hoeksema, and K. L. Harvey. Observations of the sun's magnetic field during the recent solar maximum. *Journal of Geophysical Research: Space Physics*, 108(A1):3.